Performance of DSSC with Cu Doped TiO_2 Electrode Prepared by Dip Coating Technique

L. B. Patle, A. L. Chaudhari*

Abstract— Dye Sensitized Solar Cells were fabricated using pure and Cu doped TiO_2 electrodes with 1, 2 & 3 wt % of Cu contents. The electrodes were prepared by spin coated TiO_2 blocking layer followed by co-precipitation dip coated porous TiO_2 layer. The structural analysis was carried out by XRD (Bruker D8 Cu-$K_{\alpha 1}$) and confirmed the crystalline anatase tetragonal structure. The UV-Vis Spectroscopy analysis was carried out and found that incorporation of Cu^{2+} into titanium affects the band gap of TiO_2. Field Emission Scanning Electron Microscopic (FE-SEM) analysis indicating the Cu content is affecting the porosity of film and hence conversion efficiency of DSSC. The performance of Dye Sensitized Solar cells (DSSCs) were investigated with chemically absorbed Ruthenium N719 dye electrode under light illumination with standard solar simulator (AM 1.5G, 100mW/cm^2). The short circuit current density (J_{sc}) reduces by increasing Cu concentration while open circuit voltage (V_{oc}) shows variations.

Index Terms— Cu Doped TiO2, Dip Coating, Porosity, DSSC, Open Circuit Voltage.

1 Introduction

THE wide band gap semiconductors are intensively becoming popular in sensitized solar cells since Michael Gratzel and co-workers reported low cast high efficient dye sensitized solar cells (DSSCs) [1]. The dye sensitized solar cell is becoming alternative of conventional energy sources due to its low cost as compare to silicon solar cells and simplicity of its manufacturing [2]. The DSSC consists of dye sensitized semiconductor electrode on transparent conducting oxide (TCO) electrode, I^-/I^{-3} redox electrolyte and platinum counter electrode. Commonly TCOs are fluorine doped tin oxide (FTO) or indium tin oxide (ITO) on glass or plastic substrates used in DSSCs. Under light illumination the electrons of the adsorbed dyes excited and injected into the conduction band of semiconductor. Injected electrons diffuse from the semiconductor to transparent conducting oxide interface where electron flows through external load [3]. For the semiconductor photo electrodes many wide band gap semiconductors such as ZnO, TiO_2, SnO_2, and Nb_2O_5 etc are commonly used [4-7]. Among these TiO_2 is most popular semiconductor material for its relatively high reactivity, chemical stability and excellent charge transport ability [8]. Using the anatase TiO_2 photo electrode the photoelectric conversion efficiency (η) of the DSSC has been reported 12% [9].

The heart of the DSSC is mesoporous TiO_2 electrode which plays fundamental role for photon to current conversion process. Many researchers are working to modify the properties of TiO_2 electrode such as surface morphology, conduction band position, driving force of electron injection and trap/defect level distribution etc, in order to get better light to current conversion efficiency. To enlarge the driving force of electron injection for a given dye with an insufficiently high lowest unoccupied molecular orbit (LUMO), fine-tuning of the conduction band edge of TiO_2 positively is a feasible strategy to improve the conversion efficiency and J_{sc}. In order to modify above mentioned properties a commonly adopted method is doping of metal atoms into TiO_2 semiconductor [10]. Many researchers have tried to dope different metal atoms such as Mn and Co [11], Nb [12], Sn [8], Fe [13], W [14], N [15] etc. in order to optimize the properties of TiO_2 and enhance the photon to current conversion efficiency. Apart from doping of metal atoms many efforts have been made to change the morphology, shape and size of TiO_2 nanoparticles used for DSSCs. B.R. Sankapal et al. reported TiO_2 multi wall nano tubes nanocomposites in order to enhance super capacitance of TiO_2 electrode [16], Ahmed El Ruby Mohamed et.al reported TiO_2 nanotube arrays [17], Zhuoran Wang et al reported Multilayer TiO_2 nanorods [18], in order to enhance active surface area for dye absorption.

In this article, Cu doped TiO_2 porous films deposited by dip coating method, which is novel step toward enhancing the porosity of the film. The doping of Cu was confirmed by x-ray diffraction (XRD) and EDAX. The objective of this article is to investigate the effect of copper doping on band gap of TiO_2 semiconductor and porosity of the film. The porosity of the film was evaluated by SEM images using the procedure used by M. Rosi et al, reported by Mukhtar Effendi and Bilalodin [19]. Further to investigate the performance of DSSC with TiO_2 photo electrode by copper dopant the device performance of the solar cell is evaluated in terms of cell efficiency (η) and fill factor (FF) expressed as:

$$\eta = \frac{I_{SC} \times V_{OC} \times FF}{Pin} \quad (1)$$

$$FF = \frac{I_M \times V_M}{I_{SC} \times V_{OC}} \quad (2)$$

Where J_{SC} is the short-circuit current density (mAcm^{-2}), V_{OC}

- *L.B.Patle is currently pursuing PhD degree program in electronic science in North Maharashtra University, Jalgaon, India. E-mail: lalchand.patle@gmail.com*
- *A.L.Chaudhari is Professor in the department of electronics, MGSM's ASC College Chopda Dist: Jalgaon, India. E-mail: chaudharial@yahoo.co.uk*

the open-circuit voltage (V_{OC}), and P_{in} the incident light power. J_{max} and V_{max} correspond to maximum current density and maximum voltage values respectively [20].

2 EXPERIMENTAL

2.1 Materials

Titanium Tetra Isopropoxide (TTIP) (99%) from Sigma Aldrich and Copper Acetate from Merck reagents of analytical grade without further purification were used to prepare pure and Cu doped TiO_2 electrode using dip coating method. Double distilled water and hydrogen peroxide were used as solvents and purified glycerol was used as binder.

2.2 Sample Preparation

TiO_2 blocking layer was prepared by sol-gel spin coating method on FTO glass substrates (sheet resistance 15 Ω per sq and optical transmission above 95%). Prior to deposition, the FTO coated conducting glass substrate was digressed in nitric acid for 30 sec, cleaned with acetone and soap solution, further rinsed in distilled water and dried in UV light. For the blocking layer, solution "a" was prepared by mixing 40ml TTIP and 60ml absolute ethanol and solution "b" was prepared by mixing 15 ml acetone and 30 ml absolute ethanol. Both solutions were stirred for 10 minutes and sequentially mixed the solution "b" in solution "a". The mixture was stirred for one hour at room temperature to form insoluble gel and kept for 24 hours.

Further the gel was probe sonicated for 10 minutes with 20 kHz frequency to obtain homogenous TiO_2 gel. The gel was dropped on FTO substrate and sequentially spun at 500, 2000 and 5000 rpm for 20 sec, 120 sec and 30 sec respectively to spreading, maintaining the uniform thickness and drying purpose. The deposited film was annealed at 250°C for 30 minutes and finally TiO_2 thin film was obtained.

2.3 Preparation of TiO_2 mesoporous film and Cell fabrication

To prepare pure and Cu doped TiO_2 mesoporous films, the TTIP was dissolved into distilled water for 1M solution with continuous stirring for half an hour. Another solution of copper acetate in distilled water was prepared separately for 1, 2 and 3 wt. % of copper concentration. The solution of copper acetate further added drop wise into TTIP solution for half an hour and the solution was kept for rigorous stirring for 2 hours. The obtained precipitate was filtered and washed with water for several times and found white precipitate. The 20ml H_2O_2 was further mixed with white precipitate and got transparent orange solution. This solution was further diluted with distilled water and color changed from orange to yellow. The solution was kept for 2 days in order to get appropriate viscosity of the solution for film deposition. The spin coated thin film (back covered by ticso tape) further dipped in titanium solution and pulled out with uniform pulling rate 1mm/s and dried at 100°C temperature for 5 minutes. This process was repeated for ten cycles in order to get film thick enough for DSSC application. The deposited films further annealed at 450°C in muffle furnace for 2 hrs. The remaining solution was further filtered, washed with distilled water several times and dried at 100°C temperature in air. Then precipitate was calcined at 450°C for 6 hours to obtain pure and Cu doped TiO_2 nanoparticles.

The prepared film thickness was measured by a surface profiler and found 8 - 9 μm thick. The prepared electrodes were immersed in 0.5 mM ruthenium complex *cis* - diisothiocyanato-bis (2, 2′-bipyridyl-4, 4′-dicarboxylato) Ruthenium(II) bis (tetrabutylammonium) in ethanol for 24 hours. A mixture of 0.1M Lithium iodide, 0.05M I_2, 0.6M I, 2-dimethyl-3-n-propylimidazolium iodide and 0.1M tert-butylpyridine in dehydrated acetonitrile was redox electrolyte. The platinum coated FTO glass (from solaronix) was used as counter electrode. The device performance was tested on keithley Source meter (Keithley Instruments, Inc. Model 2420) under dark and illumination. The simulated light supplied from AM 1.5 G solar simulator (Newport Co.). The incident light intensity was 1000W/m^2 condition calibrated with standard Si Solar cell.

3 RESULTS AND DISCUSSION

3.3 X-ray analysis

Figure 1 shows the X-ray diffraction patterns of pure and Cu doped TiO_2 nanoparticles determined by X-ray diffractometer (Bruker D8 Advance Diffractometer) with CuK_{a1} radiations (λ = 1.5418 Å) in the 2θ range of 20° to 80° at room temperature. The dominant peak is obtained at 2θ = 25.387 corresponding to (101) plane of TiO_2. Rest of the peaks can be indexed to the anatase phase (JCPDS no. 73-1764) which confirms prepared TiO_2 is anatase tetragonal structure. Further it is observed that in pure TiO_2 samples some peaks of rutile structure are present (2θ = 27.479 and 36.166 corresponds to (110) and (101) respectively is matching with JCPDS data (84-1284)). It may be due to the annealing temperature was at 450°C. Yan Hua Peng et.al reported that at 600°C temperature mixture of anatase and rutile phase are present [21]. As the Cu concentration increases intensity of rutile peaks reduces. It may be due to the active surface area increases by increasing copper concentration and by increasing active surface area rutile converts into anatase phase [22]. From the x-ray diffraction pattern all the peaks can be assigned to TiO_2 crystal and the samples do not contained any peaks of copper oxide which are reported in the literature (2θ=35.6°C and 38.7°C) [23]. It is also observed that the diffraction peaks shift to lower theta values with increasing Cu concentration. This shifting of peaks may be due to the ionic radius of Cu^{2+} (0.73 Å) is greater than that of Ti^{4+} (0.61 Å). The shifting of peaks to lower theta value is more obvious in higher theta with increasing Cu contents.

The anatase tetragonal lattice parameters such as the distance between adjacent planes in the miller indices 'd' is calculated from Braggs equation $n\boldsymbol{\lambda}=2d\sin\theta$ and lattice constant 'a' and 'c' are calculated from Lattice Geometry equations [24]. The particle size of pure and Cu doped TiO_2 sample were calculated by the x-ray line broadening technique using Debye Scherer equation ($D=k\lambda/\beta\cos\theta$). The lattice parameters and grain size of pure and Cu doped TiO_2 nanoparticles are summarized in table 1. Figure 2 shows the effect of Cu concentration on the TiO_2 nanoparticles. As the doping level of Cu concentration increases, the grain size goes to decrease. This may be due to

dopant ions of Cu and sintering temperature which inhibits the crystal growth during heat treatment.

TABLE 1: PARAMETERS AND GRAIN SIZE OF PURE AND CU DOPED TIO₂ NANOPARTICLES

Sample	$d_{(hkl)}$ at 2θ =25.38	Lattice parameter in (A°)		Volume in $(A°)^3$	Grain size D (nm)
		a	c		
Pure TiO_2	3.5056	3.7770	9.6119	137.1208	17.84
1% Cu TiO_2	3.4957	3.7775	9.4547	134.9139	17.35
2% Cu TiO_2	3.5131	3.7798	9.5390	136.2826	13.09
3% Cu TiO_2	3.5031	3.7754	9.5631	136.3090	9.44

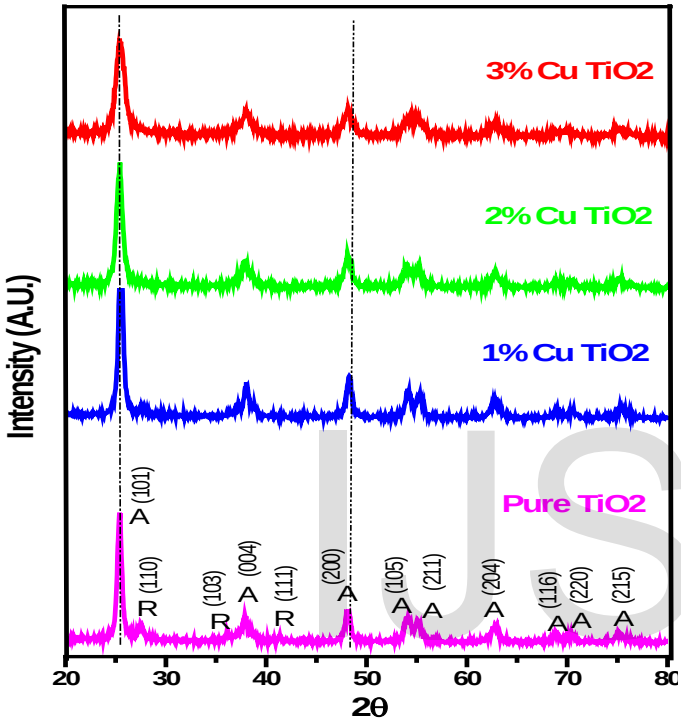

Figure 1: XRD pattern of pure and Cu doped TiO_2 nanoparticles

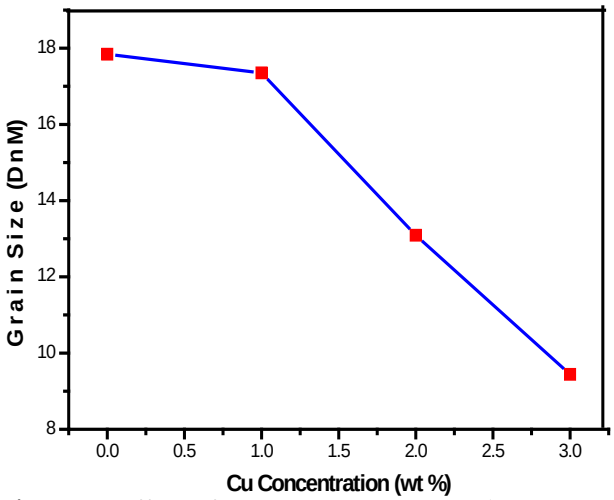

Figure 2: Effect of Cu concentration on the grain size of TiO_2

3.3 *Optical analysis*

Figure 3 shows the UV-vis spectra of pure and Cu doped TiO_2 samples recorded in the wavelength range 200-800 nm at room temperature. The optical absorption of Cu doped TiO_2 shifted toward lower energy in the visible range as the Cu concentration increases. This indicates the band gap is narrowing upon doping concentration. The band gap of prepared sample was calculated by Tauc's equation given as $(\alpha h\nu) = A(h\nu - E_g)^n$ [25]. Where 'α' was obtained from absorption data, 'A' is an energy – independent constant, '$h\nu$' is the photon energy (h is plank constant and ν is wave number) and 'n' depends on type of transition. The graph has been plotted between $(\alpha h\nu)^2$ versus energy ($h\nu$). From the graph it is found that the absorption edge of Ti_{1-x} Cu_xO samples display a gradual shift from blue to red shift with their bandgap which decrease from 3.33 eV to 2.98 eV. This consecutive shifting of absorption peak from red shift to blue shift is consistent with the shift of diffraction peaks from higher angle to lower angle shown in figure (1). The band gap is one of the factors affecting the open circuit voltage of the DSSCs hence the presence of Cu in the semiconductor structure may leads to increase in the open circuit voltage of the DSSCs [26].

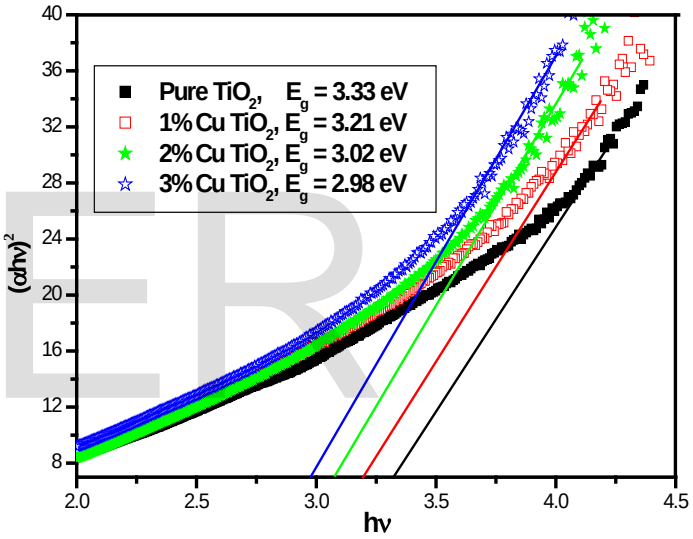

Figure 3: $(\alpha h\nu)^2$ versus Energy of Pure and Cu doped TiO_2

3.4 *Surface morphology of TiO_2 electrode*

The Surface morphology of TiO_2 electrodes were carried out by field emission scanning electron microscope (FESEM) is shown in figure 4. The TiO_2 blocking layer (figure 4.a) deposited by spin coating illustrates a homogeneous compact layer without cracks. Figure 4(a) shows that the compact layer deposited is uniform and granular crystalline with average grain size about 22 nm. Figure 4(b - d) shows the SEM images of pure and Cu doped TiO_2 film prepared by dip coating method. The overall porous surface area of pure and Cu doped TiO_2 film can be observed, which provides high surface area for the further dye absorption. The size of porous area is calculated using the procedure reported by Mukhtar Effendi et.al [19]. The porosity of the film increases by increasing Cu concentration, summarized in figure 5. This may be due to the defects will be increased by increase in doping concentration [12]. Further this was observed that after increasing Cu concentration the agglomeration of the particles takes place and starts to peeled off the TiO_2 film. Figure 6(a - b) shows the

EDAX data of film with 1 and 2 wt % of Cu doped TiO_2 film which confirms the doping concentration of copper into TiO_2.

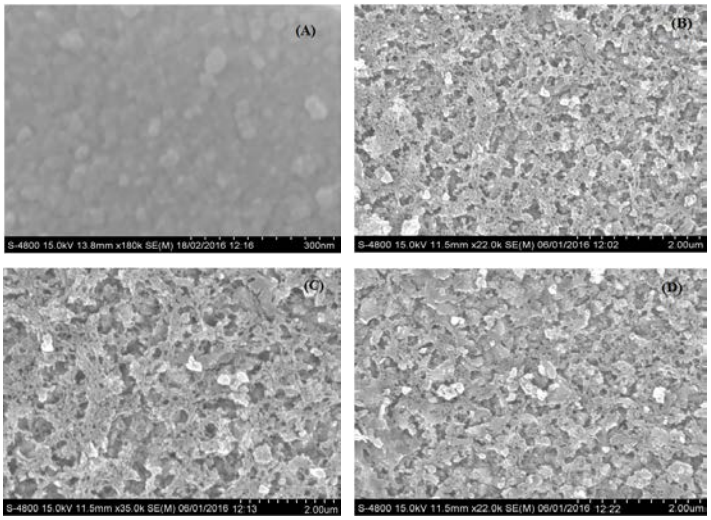

Figure 4: FESEM TiO_2 blocking layer thin film (a), Pure TiO_2 porous film (b), 1 % Cu doped TiO_2 (c), 2% Cu Doped TiO_2 (d)

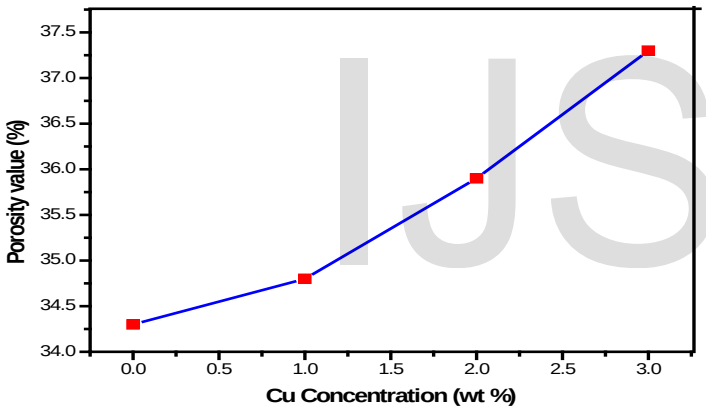

Figure 5: Effect of Cu concentration of Porosity of film

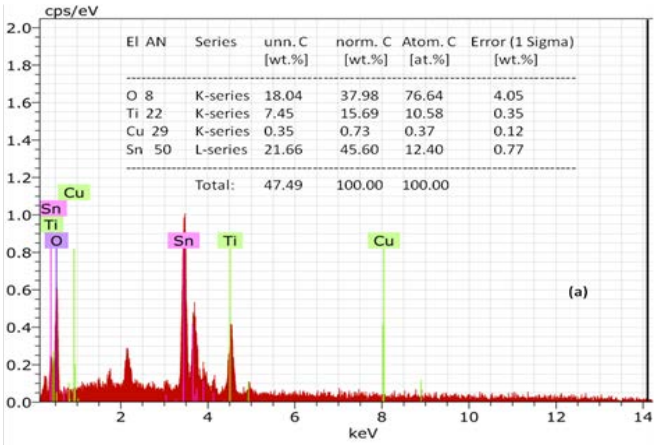

Figure 6: EDAX data of (a) 1% Cu Doped TiO_2, and (b) 2% Cu doped TiO_2

3.5 Device performance

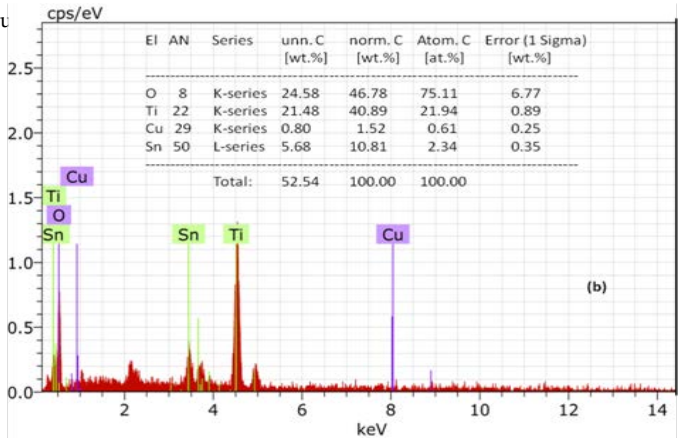

The constructed dye sensitized solar cell has a structure FTO/compact TiO_2/porous TiO_2/dye/electrolyte/platinum/FTO shown in figure 7(a). From the voltage to current density plot we analyze the photovoltaic characteristics of device. The parameters such as open circuit voltage (V_{oc}), short circuit current (J_{sc}), field factor (FF) and efficiency (η) were calculated from the recorded J-V data which are summarized in table 2. From the figure 8(a) it can be observed that upto 2% of copper concentration V_{oc} increases. The increase in open circuit voltage may due to the decrease in band gap. For 3% Cu concentration the open circuit voltage suddenly decreases. The open circuit voltage is the difference between the flat band potential and the redox potential of electrolyte. A. E. Shalan et.al reported that V_{oc} is also related to trap density which causes the charge recombination [11]. M. I. Rosenbluth et al conclude that the recombination is dynamic cause for decrease in open circuit voltage. [27]. By increasing Cu concentration the flat band potential may shift positive and trap density may increase due to which the recombination increases and hence decreases the open circuit voltage. The decrease in short circuit current has several causes such as impurities of Cu present on the surface of the semiconductor may cover active surface area of TiO_2 and after increasing Cu concentration the electron concentration increases etc. The effect of enhancement of electron concentration can be understand by the theoretical model for electrical conductivity $\sigma = ne\mu$. Here e represents elementary charge, $\mathbf{n}$ represents concentration of electron and $\boldsymbol{\mu}$ represents the electron mobility. Xujie Lu et al reported the increase in electron concentration enhances the electron conductivity and improve electron transport efficiency which increases the photocurrent density [12]. However with respect to defect concentration the electron mobility decreases rapidly due to electron scattering by defects. More defects increases charge recombination, which is the dominant factor for copper concentration. Since copper is highly sensitive material and increases the defects in TiO_2 electrode.

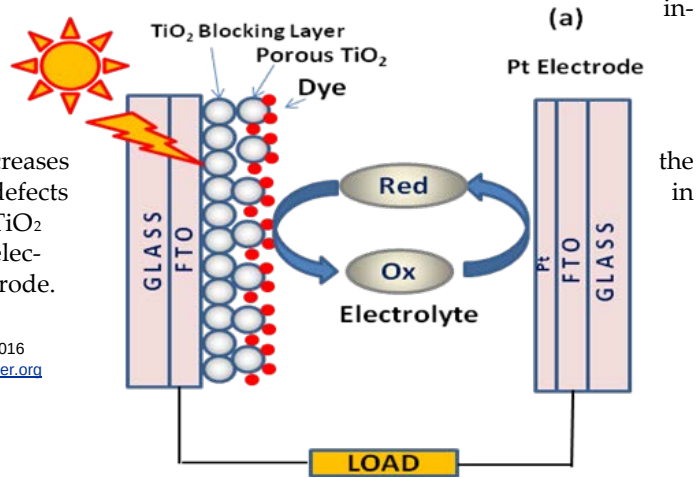

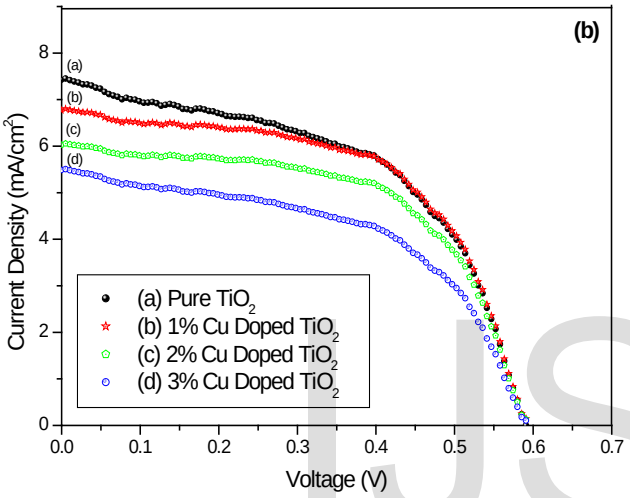

Figure 7: (a) Schematic illustration of device, (b) J-V Characteristics of device for pure and Cu doped TiO_2 photo electrode.

From the SEM analysis it may conclude that by increasing copper concentration the defects are increasing in TiO_2 film and hence the photocurrent density decreases. The photon to current conversion efficiency (η) goes to decrease consistently with increasing Cu contents. This may be due to increase in concentration of impurities with increasing Cu contents. These increased impurities could produces blockage around the active surface area of TiO_2 and act as charge trapping site for the electron hole recombination. The decrement in efficiency is also consistent with grain size.

Table 2: Photovoltaic characteristics of DSSCs made with pure and Cu doped TiO_2 photo electrode.

Photo electrode	V_{oc} (Volt)	J_{sc} (mA cm^{-1})	FF	η (%)
Pure TiO_2	0.5916	7.4814	0.5194	2.299
1% Cu-TiO_2	0.5917	6.8461	0.5637	2.283
2% CuTiO_2	0.5942	6.0584	0.5717	2.058
3% Cu-TiO_2	0.5866	5.5277	0.5159	1.673

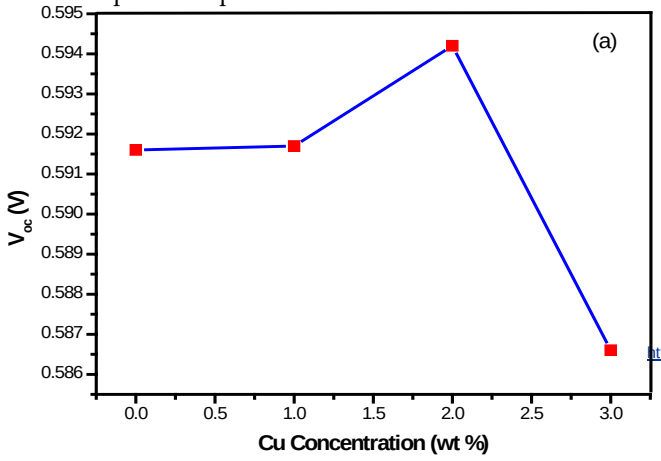

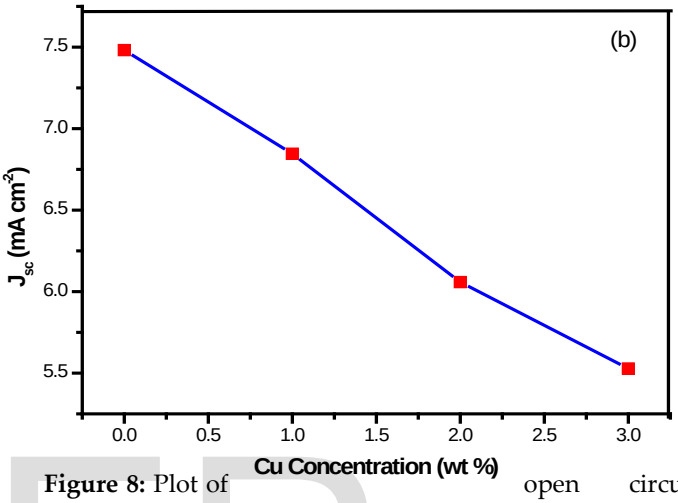

Figure 8: Plot of open circuit voltage (a) and short circuit current density (b) vs Cu Concentration

4 Conclusions

Simple, inexpensive dip coating method at room temperature is reported for deposition of pure and Cu doped TiO_2 photo electrode over spin coated compact TiO_2 blocking layer. Prepared dip coated TiO_2 semiconductor meet enough porosity for the application of DSSC. The films deposited were prepared by 10 cycles and observed thickness about 8-9 μm. The thickness could be increased by increasing cycles but when dried the coated TiO_2 film gets peeled off from the substrate. Even increasing the Cu concentration after 3% the TiO_2 film gets detached from the substrate. This shows that the adhesion of film is very poor for more than 10 cycles as well as Cu concentration more than 3%. Further the investigation has shown the effect of Cu doping in TiO_2 semiconductor reduces the band gap of TiO_2 upto 10%. This decrease in band gap energy of TiO_2 semiconductor corresponds to increase in open circuit voltage of the DSSC. On the other hand increase in Cu concentration the short circuit current and photon to current conversion efficiency of the DSSC decreases.

5 Acknowledgement

L.B. Patle gratefully acknowledges the University Grants Commission WRO Pune for financial support under Minor Research Project [Ref: UGC47-815/13(WRO) dated: 23 May 2014]. Further author extends his highly indebted to Prof. P. K. Labhane and Prof. V. R. Huse for their guidance and providing necessary information.

REFERENCES

[1] B. O Regan, M. Gratzel, A low cast high efficiency solar cell based on dye sensitized colloidal TiO_2 films, *Nature,* **1991,** *353,* 737–740.

[2] Mao, Samuel S., and Xiaobo Chen., Selected nanotechnologies for renewable energy applications, *International journal of energy research,* **2007,** *31*, 6-7, 619-636. **DOI:** 10.1002/er.1283

[3] M. Hamadanian, V. Jabbari, A. Gravand, M. Asad, Band gap engineering of TiO_2 nanostructure based dye solar cells (DSCs) fabricated via electrophoresis, *surface & Coatings Technology,* **2012,** 206, 4531-4538.
DOI: 10.1016/j.surfcoat.2012.03.017

[4] Jensen, R. A., Van Ryswyk, H., She, C. X., Szarko J. M., Chen L. X., Hupp J. T., Dye-sensitized solar cells: sensitizer-dependent injection into ZnO nanotube electrodes, *American Chemical Society*, **2010**, 26 (3), 1401−1404.
DOI: 10.1021/la902991z

[5] Nazeeruddin, M.K., De Angelis, F., Fantacci, S., Selloni, A. , Viscardi, G., Liska, P., Ito, S., Takeru, B., Grätzel, M., Combined experimental and DFT-TDDFT computational study of photoelectrochemical cell ruthenium sensitizers, *J. Am. Chem. Soc.*, **2005**, 127, 16835-16847.
DOI: 10.1021/ja0524671

[6] Hara, K.; Horiguchi, T.; Kinoshita, T.; Sayama, K.; Sugihara, H.; Arakawa, H., Highly Efficient Photon to Electron Conversion with mercurochrome Sensitized nanoporous oxide semiconductor solar cell, *Sol. Energy Mater. Sol. Cells,* **2000**, 64 (2), 115−134.

[7] Snaith, H. J.; Ducati, C., SnO_2-Based Dye-Sensitized Hybrid Solar Cells Exhibiting Near Unity Absorbed Photon-to-Electron Conversion Efficiency, *Nano lett.* **2010**, 10 (4), 1259−1265.
DOI: 10.1021/nl903809r

[8] Yandong Duan, Nianqing Fu, Qiuping Liu, Yanyan Fang, Xiaowen Zhou, Jingbo Zhang, and Yuan Lin, Sn-Doped TiO_2 Photoanode for Dye-Sensitized Solar Cells, *J. Phys. Chem. C,* **2012**, 116, 8888−8893.
DOI: 10.1021/jp212517k

[9] Qingjiang Yu, Yinghui Wang, Zhihui Yi, Ningning Zu, Jing Zhang, Min Zhang, and Peng Wang, High-Efficiency Dye-Sensitized Solar Cells: The Influence of Lithium Ions on Exciton Dissociation, Charge Recombination, and Surface States, *American Chemical Society,* **2010** VOL. 4 NO. 10, 6032 – 6038.
DOI: 10.1021/nn101384e

[10] Daniel P. Hagberg, Tomas Edvinsson, Tannia Marinado, Gerrit Boschloo, Anders Hagfeldt and Licheng Sun, A novel organic chromophore for dye-sensitized nanostructured solar cells, *The Royal Society of Chemistry* **2006**.
DOI: 10.1039/B603002E

[11] A. E. Shalan, M. M. Rashad, Incorporation of Mn^{2+} and Co^{2+} to TiO_2 nanoparticles and the performance of dye sensitized solar cell, *Applied Surface Science* 283, **2013**, 975-981**. DOI:** 10.1016/j.apsusc.2013.07.055

[12] Xujie Lu, Xinliang Mou, Jianjun Wu, Dingwen Zhang, Linlin Zhang, Fuqiang Huang, Fangfang Xu, and Sumei Huang, Improved-Performance Dye-Sensitized Solar Cells Using Nb-Doped TiO_2 Electrodes: Efficient Electron Injection and Transfer, *Adv. Funct. Mater.* **2010**, 20, 509–515.
DOI: 10.1002/adfm.200901292

[13] Moo Chin Wang, Huey Jiuan Lin, Tien Syh Yang, Characteristics and optical properties of iron (Fe^{3+}) doped titanium oxide thin films prepared by a sol gel spin coating, *Journal of Alloy and Compounds* 473, **2009**, 394-400.
DOI: 10.1016/j.jallcom.2008.05.105

[14] Xi Zhang, Fang Liu, Qiu-Liu Huang, Gang Zhou and Zhong Sheng Wang, Dye sensitized W Doped TiO_2 Solar Cells with a Tunable Conduction Band and Suppressed Charge Recombination, *J. Phy. Chem. C* **2011**, 115, 12665-12671. **DOI:** 10.1021/jp201853c

[15] Wei Qin, Songtao Lu, Xiaohong Wu, Song Wang, Dye Sensitized Solar Cell Based on N-Doped TiO_2 Electrode Prepared on Titanium, *Int. J. Electrochem. Sci.* 8, **2013**, 7984-7990.

[16] B. R. Sankapal, H. B. Gajare, D. P. Dubal, R.B. Gore, R. R. Salunkhe, H. Ahn, Presenting highest supercapacitance for TiO_2/MWNTs nanocomposites: Novel method, *Chemical Engineering Journal* 247, **2014,** 103–110.
DOI:10.1016/j.cej.2014.02.092

[17] Ahmed El Ruby Mohamed and Sohrab Rohani, Modified TiO_2 nanotube arrays (TNTAs): progressive strategies towards visible light responsive photoanode, a review, *Energy Environ. Sci.*, **2011**, 4, 1065.
DOI: 10.1039/C0EE00488J

[18] Zhuoran Wang, Sihan Ran, Bin Liu, Di Chen and Guozhen Shen, Multilayer TiO_2 nanorod cloth/nanorod array electrode for dye-sensitized solar cells and self-powered UV detectors, *Nanoscale*, **2012**, 4, 3350.
DOI: 10.1039/C2NR30440F

[19] Mukhtar Effendi and Bilalodin, Effect of Doping Fe on TiO_2 Thin Films Prepared by Spin Coating Method, *Int. Jr. of Basic & Applied Sciences IJBAS-IJENS* Vol: 12, No 02, April **2012**, 107-110.

[20] Jiawei Gong, Jing Liang, K.Sumathy, Review on dye-sensitized solar cells (DSSCs): Fundamental concepts and novel materials, *Renewable and Sustainable Energy Reviews* 16, **2012,** 5848–5860.
DOI: 10.1016/j.rser.2012.04.044

[21] Yan Hua Peng, Gui-fang Huang, Wei Qing Huang, Visible light absorption and photocatalytic activity of Cr doped TiO_2 nanocrystal film, *Advance Powder Technology* **2010**. **DOI**: 10.1016/j.apt.2010.11.006

[22] Akihiko Kudo, Yugo Miseki, Heterogeneous photocatalyst materials for water splitting, *Chem. Soc. Rev.*, **2009**, 38, 253-278.
DOI: 10.1039/B800489G

[23] L.S. Yoong, F.K. Chong, Binay K. Dutta, Development of copper-doped TiO2 photocatalyst for hydrogen production under visible light, *Energy* 34, **2009**, 1652–166. **DOI:**10.1016/j.energy.2009.07.024

[24] A. Khorsand Zak, W. H Abd. Majid, M. E. Abrishami, RaminYousefi, X-Ray analysis of ZnO nanoparticles by Williamson Hall and size strain plot method, *Solid Sate Sciences* 13, **2011**, 251-256.
DOI: 10.1016/j.solidstatesciences.2010.11.024

[25] A.Y. El-Etre, S.M. Reda, Characterization of nanocrystalline SnO2 thin film fabricated by electrodeposition method for dye-sensitized solar cell application, *Applied Surface Science* 256, **2010,** 6601–6606.
DOI: 10.1016/j.apsusc.2010.04.055

[26] J. Navas, C. Fernandez-Lorenzo, T. Aguilar, R. Alcantara, and J. Martın-Calleja, Improving open-circuit voltage in DSSCs using Cu-doped TiO2 as a semiconductor, *Phys, Status Solidi*, **2012** No. 2, 378-385.
DOI: 10.1002/pssa.201127336

[27] M. L. Rosenbluth, N.S. Lewis, Ideal Behavior of the Open Circuit Voltage of Semiconductor Liquid Junction, *J. Phys, Chem.* **1989** 93, 3735-3740